

Research Article

Calculation Model of Rock Fracture Pressure with Multifields in the Process of Fracturing

Zhao Xiaojiao ^{1,2,3}, Qu Zhan,^{1,2,3} Xu Xiaofeng,⁴ Yu Xiaocong,⁵ Fan Heng,² and Song Xijin²

¹School of Aeronautics, Northwestern Polytechnical University, Xi'an, Shanxi, 710072, China

²School of Electronic Engineering, Xi'an Shiyou University, Xi'an, Shanxi, 710065, China

³Key Laboratory of Well Stability and Fluid and Rock Mechanics in Oil and Gas Reservoir of Shanxi Province, Xi'an, Shanxi, 710065, China

⁴Standardization and Information Center, CNPC Tubular Goods Research Institute, 710077 Xi'an, China

⁵China University of Geosciences, Wuhan, Hubei, 100083, China

Correspondence should be addressed to Zhao Xiaojiao; zhaoxsyu@qq.com

Received 5 June 2018; Accepted 2 October 2018; Published 17 October 2018

Academic Editor: Gilberto Espinosa-Paredes

Copyright © 2018 Zhao Xiaojiao et al. This is an open access article distributed under the Creative Commons Attribution License, which permits unrestricted use, distribution, and reproduction in any medium, provided the original work is properly cited.

In this paper, a comprehensive model to calculate the rock fracture pressure by the theory of double effective stress of porous medium is established, which considers such effective factors as the crustal stress field, hydration stress field, temperature field, tectonic stress field, the porosity of rock, and additional stress field generated by seepage of drilling fluid. This new model is applicable to predict the fracture pressure of different types of rocks. Using the experimental parameters of field fracturing and the experimental results of three-axis compression of rock cores with different water contents, we may get the calculated fracture pressure. Compared with the measured fracture pressure in the oilfield, the result calculated in the present study shows good agreement. Besides, the effects of water contents on the tensile strength and fracture pressure are analyzed. Results show that both the tensile strength and fracture pressure decrease with the increase of water contents, which is due to the reduction of the mechanical properties of rocks by hydration.

1. Introduction

Formation fracture pressure refers to the pressure which causes formation fracture or original fracture to be reopened under the action of mud string pressure in the open hole well. It is widely used in drilling well structure, well control design and operation, fracturing, and increasing production in oilfield production process. In order to meet the society's demand for oil and gas resources, unconventional oil and gas resources have been explored and developed. The geological structure is becoming complex, which is affected by the chemical field [1–3], temperature field [4, 5], seepage field [6], and tectonic stress [7]. How to obtain accurate formation fracture pressure and guide production become more critical and difficult [8].

Scholars have put forward many models to predict the formation fracture pressure. Anderson [9] used the well logs to calculate fracture pressure. Li [10] proposed a fracture

pressure model by the double effective stress theory [11], which combines the advantages of both H-F fracture pressure formula [12] and the H-W fracture pressure formula [13]; the double effective stress theory has been widely applied in many fields such as oil, rock, coal, and foundation engineering [14–16]. Compared with Li's model, Huang [7] considered the relationship between overlying stress and depth, tectonic stress and rock strength. However, both Li's model and Huang's model did not consider the influence of chemical and temperature fields. Yan [17] built a simple model for calculating the fracture pressure considering hydration stress, which improved the prediction accuracy. Li [4] established the mathematical model of additional thermal stress produced by temperature change on the shaft lining and proposed the calculation method of additional fracture pressure caused by temperature change. Deng [18] established a fracture pressure calculation model for high temperature and high pressure formation, which took into account the variation of

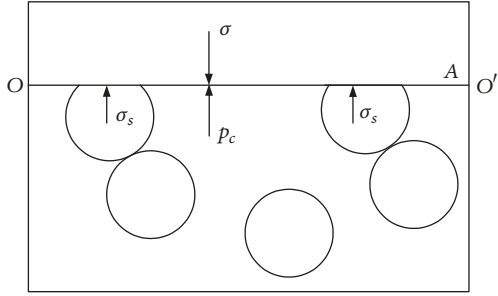


FIGURE 1: The body effective stress diagram of rocks [11].

wellbore temperature and wellbore permeability, but it did not consider the influence of chemical field and it is only fit for sandstone.

In this paper, a comprehensive model to calculate the rock fracture pressure by the theory of double effective stress of porous medium is established, which fully considers the deformation mechanism and material structure of the porous medium. Besides, this model proposed in this paper takes into account important effective factors such as the ground stress field, the inner pressure of the wellbore, chemical field, temperature field, tectonic stress field, porosity of rocks, seepage of the penetrating fluid, and the double effective stress. This new model is applicable to predict the fracture pressure of different types of rocks by changing the parameters of rocks in the model.

2. Deduction of the Rock Fracture Pressure Model

2.1. Effective Stress of Rock. Rock is composed of a large number of solid particles and intergranular pores. Usually the pores of rock are saturated with fluid, so the rock is affected by both external and internal pressures. It makes the stress state of rock more complicated, so many theories of solid mechanics cannot be directly applied to the study of rock mechanics; the stress state of rock could be simplified to obtain the effective stress of rock. There are two effective stresses in the rock [19]: the body effective stress and the structure effective stress.

2.1.1. The Body Effective Stress. Rocks are affected by the external stress σ and internal stress p_c ; meanwhile, there are skeleton stresses σ_s at any point in the rock in the continuum. However, the skeleton stress σ_s does not exist independently; it is affected by both internal and external stresses of rock; that is, σ_s is a function of σ and p_c ; σ_s is not measurable but can be calculated by formula.

From Figure 1, the external stress of the rock above the arbitrary surface OO' is σ ; the action area of the external stress is A . Therefore, the total external force on the rock is σA . The skeleton stress below the surface QQ' is σ_s ; the action area of the skeleton stress is $(1 - \phi_c)A$. According to the static equilibrium principle, the upper and lower forces exerted by the skeleton on the surface OO' should be equal.

$$\sigma A = (1 - \phi) \sigma_s A + \phi p_c A. \quad (1)$$

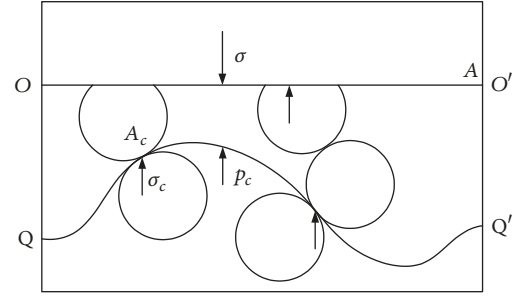


FIGURE 2: The structure effective stress diagram of rocks [11].

Equation (1) can be simplified to

$$\sigma = (1 - \phi) \sigma_s + \phi p_c. \quad (2)$$

σ is the external stress of the rock above the arbitrary interface OO' , MPa; ϕ is the porosity of rock; σ_s is the skeleton stress under the arbitrary interface OO' , MPa; p_c is the rock internal stress, MPa. By (2), we can obtain the skeleton stress. When we convert it to the cross section area of the whole rock, the body effective stress σ_{ep} that determines the body deformation of the rock is obtained.

$$\sigma_{ep} = \sigma - \phi p_c. \quad (3)$$

2.1.2. The Structure Effective Stress. The contact stress σ_c among rock skeleton particles determines the structural deformation of rocks; it is the result of the interaction of both the internal and external stresses of the rock; that is, σ_c is a function of σ and p_c ; it is not measurable but can be calculated by formula.

From Figure 2, the skeleton stress below the surface QQ' is σ_c ; the action area of the skeleton stress is $(1 - \phi_c)A$; the total contact force of vertical stress to the surface QQ' is $(1 - \phi_c)\sigma_c A$. The pore pressure below the surface QQ' is p_c ; the action area of the vertical force of pore pressure is $\phi_c A$, so the total force of the fluid in pore on the surface QQ' is $\phi_c p_c A$.

When the surface QQ' tends to the surface OO' , according to the static equilibrium principle, we can get

$$\sigma A = (1 - \phi_c) \sigma_c A + \phi_c p_c A. \quad (4)$$

Equation (4) can be simplified to

$$\sigma = (1 - \phi_c) \sigma_c + \phi_c p_c. \quad (5)$$

σ_c is the vertical contact stress among rock skeleton particles under the arbitrary surface OO' , MPa; ϕ_c is the rock contact porosity, %.

By (5), we can obtain the contact stress. When we convert it to the cross section area of the whole rock, the structure effective stress that determines the structural deformation of rock is obtained.

$$\sigma_{es} = \sigma - \phi_c p_c. \quad (6)$$

σ_{es} is the structure stress of rock, MPa. When $\phi_c \rightarrow 0$, $\phi \rightarrow 0$, the pore characteristics of rocks disappear, and rocks

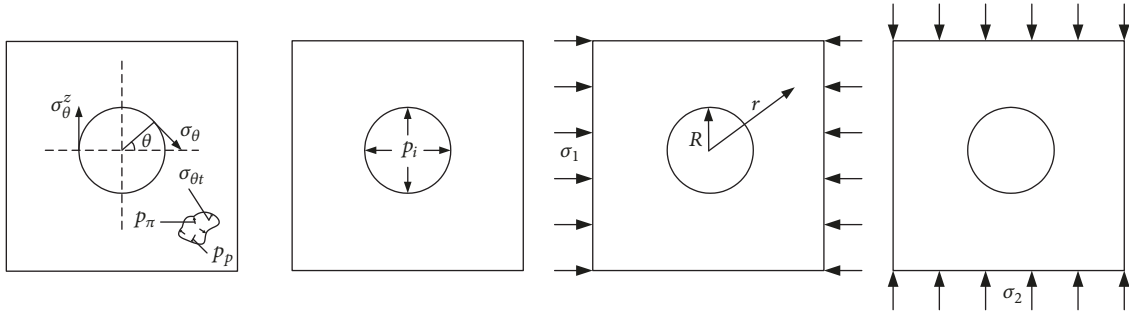


FIGURE 3: Stress state around wellbore.

tend to be ordinary solid materials. At this time, both the body effective stress and the structure effective stress tend to the external stress of rock. When $p_c \rightarrow 0$, (6) shows that there is no fluid in the rock. At this time, both the body effective stress and the structure effective stress tend to be the external stress of rock, too. When $\varphi_c \rightarrow 1$, (6) shows that the rock tends to be the loose medium. At this time, the structure effective stress formula is the Terzaghi effective stress.

$$\sigma_{es} = \sigma - p_c. \quad (7)$$

2.2. Wellbore Stress Field Model. Vertical wellbore can be regarded as a circular hole on the infinite plane (see Figure 3). It is subjected to horizontal stress in two directions σ_1 and σ_2 in this plane, overpressure on the vertical direction, hydration stress p_π , temperature variable stress $\sigma_{\theta t}$, pore pressure of rock p_p , and the minimum circumferential stresses on the shaft lining σ_θ^z . It is supposed that the formation is an isotropic linear elastic porous medium; the rock around the borehole is in a plane strain state [18]. The stress model of the wellbore wall is shown in Figure 3.

p_i is the liquid pressure in well bore, MPa; σ_1 is the maximum horizontal stress, MPa; σ_2 is the minimum horizontal stress, MPa; R is the radius of the borehole, m; r is the radius of one point from the borehole axis to the stratum, m; θ is the well circumferential angle [20].

2.3. The Circumferential Stress Generated by Ground Stress on the Wall of a Well. Due to the existence of the wellbore, the ground stress and its distribution in the stratum will change. The circumferential stress at any point in the stratum is given by the elastic mechanics.

$$\begin{aligned} \sigma_{\theta 1} = & -\frac{R^2}{r^2} p_i + \frac{(\sigma_1 + \sigma_2)}{2} \left(1 + \frac{R^2}{r^2} \right) \\ & - \frac{(\sigma_1 - \sigma_2)}{2} \left(1 + \frac{3R^4}{r^4} \right) \cos 2\theta. \end{aligned} \quad (8)$$

$\sigma_{\theta 1}$ is the circumferential stress caused by ground stress, MPa. When $r = R$ and $\theta = 0^\circ$ or $\theta = 180^\circ$, the minimum value of the circumferential stress in wellbore is [6]

$$\sigma_{\theta 1} = 3\sigma_2 - \sigma_1. \quad (9)$$

2.4. The Circumferential Stress Generated by the Inner Pressure of the Wellbore. During the fracturing process, high pressure fluids are injected into the wellbore, so the pressure in the wellbore increases rapidly. The circumferential stress is produced on the shaft lining. If we regard the formation around the wellbore as an infinite wall cylinder, the circumferential stress generated by wellbore pressure is obtained by elasticity.

$$\sigma_{\theta 2} = \frac{p_e r_e^2 - p_i R^2}{r_e^2 - R^2} + \frac{(p_e - p_i) r_e^2 R^2}{r^2 (r_e^2 - R^2)}. \quad (10)$$

$\sigma_{\theta 2}$ is the circumferential stress generated by the wellbore inner pressure, MPa; p_e is the outer boundary pressure of the thick wall cylinder, $p_e = 0$; r_e is the outer boundary radius of the thick wall cylinder, $r_e \rightarrow \infty$. When $r_e \rightarrow \infty$, $p_e = 0$, and $r = R$, (10) can be written as [6]

$$\sigma_{\theta 2} = -p_i. \quad (11)$$

2.5. The Circumferential Stress Generated by the Penetrating Fluid and the Body Effective Stress. The radial flow of drilling fluid in the formation will generate additional circumferential stresses around the wellbore [21]. As the body effective stress is shown in (3), the increment and distribution of the in situ stress caused by the increment of pore pressure are [10]

$$\begin{aligned} \sigma_{\theta 3} = & -\frac{(1-2\mu)}{2(1-\mu)} \phi \left[\frac{1}{r^2} \int_R^r (p - p_p) r dr \right. \\ & \left. + \frac{r^2 + R^2}{r^2 (r_e^2 - R^2)} \int_R^{r_e} (p - p_p) r dr - (p - p_p) \right]. \end{aligned} \quad (12)$$

p is the pore pressure at any point in the formation, MPa; p_p is the pore pressure of fluid in the stratum, MPa. For thick wall cylinders, $r_e \rightarrow \infty$. When $r = R$, $p = p_i$. Then the circumferential stress due to the increase of pore pressure is got [10].

$$\sigma_{\theta 3} = \phi \frac{(1-2\mu)}{2(1-\mu)} (p_i - p_p). \quad (13)$$

$\sigma_{\theta 3}$ is the circumferential stress generated by the fluid penetrating into the shaft lining, MPa; μ is a Poisson ratio; ϕ is the porosity of rock, %.

2.6. *The Circumferential Stress Generated by Chemical Field.* Drilling fluid enters the wellbore through the action of hydraulic pressure difference and permeability potential difference. The rock around the wellbore is prone to hydration when it encounters water; hydration can reduce the rock strength and cause instability of the wellbore [6, 22, 23]. Chenevert [24] regarded the shaft lining as a semipermeable membrane; he used hydrostatic pressure to represent hydration stress. The formula is as follows:

$$\sigma_{\theta 4} = p_{\pi} = -I_m \frac{R'T}{\bar{V}} \ln \frac{(A_w)_m}{(A_w)_{sh}} \times 10^{-6}. \quad (14)$$

$\sigma_{\theta 4} = p_{\pi}$ is the hydration stress, MPa; R' is the gas constant, $\text{J} \cdot \text{mol}^{-1} \cdot \text{K}^{-1}$; T is the absolute temperature, K; I_m is the membrane permeable efficiency; \bar{V} is the partial molar volume of pure water, $\text{m}^3 \cdot \text{mol}^{-1}$; $(A_w)_m$ is the liquid activity of water entering the formation; $(A_w)_{sh}$ is the activity of water in formation [20].

2.7. *The Circumferential Stress Generated by Temperature Field.* Maury [5] and Boas [25] thought that the temperature change of shaft wall could cause instability of shaft lining. When the drilling fluid circulates, the upper wellbore surrounding rock is heated. When the circulation stops, the lower wellbore surrounding rock is heated again, so the wellbore surrounding rock is heated and expanded. However, it is restricted by the wellbore fluid column pressure and the wellbore surrounding rock cannot expand freely. Thus, the temperature stress will occur in the wellbore surrounding rock, which changes the circumferential stress of the surrounding rock of the shaft lining; the circumferential stress caused by the temperature stress is as follows [25, 26]:

$$\begin{aligned} \sigma_{\theta t} &= \sigma_{\theta 5} \\ &= \frac{E\alpha_m}{3(1-\mu)} \left[\frac{1}{r^2} \int_R^r T_k(r, t) r dr + T_k(r, t) \right]. \end{aligned} \quad (15)$$

$T_k(r, t) = T(r, t) - T_0$; $T_k(r, t)$ is the temperature variation field around the wellbore; α_m is the volumetric thermal expansion coefficient of rock. E is the elastic modulus of stratum rock, GPa. When $r = R$, (15) can be changed into

$$\sigma_{\theta 5} = \frac{E\alpha_m}{3(1-\mu)} [T_w - T_0]. \quad (16)$$

T_w is the temperature on the shaft lining, °C; T_0 is the temperature in the original stratum, °C.

2.8. *Total Circumferential Stress on the Wall of a Wellbore.* Because the formation rock is assumed to be an isotropic linear elastic porous medium, the stress state of the wall rock can be obtained by using the principle of linear superposition. The minimum circumferential stress on the shaft lining σ_{θ}^z is the sum of the above five stresses.

$$\begin{aligned} \sigma_{\theta}^z &= \sigma_{\theta 1} + \sigma_{\theta 2} + \sigma_{\theta 3} + \sigma_{\theta 4} + \sigma_{\theta 5} \\ &= 3\sigma_2 - \sigma_1 - p_i + \phi \frac{(1-2\mu)}{2(1-\mu)} (p_i - p_p) + p_{\pi} \\ &\quad + \frac{E\alpha_m}{3(1-\mu)} [T_w - T_0]. \end{aligned} \quad (17)$$

2.9. *The Minimum Structure Circumferential Stress.* By (6) and $p_i = p_c$, the effective stress of the total minimum circumferential structure on the shaft wall σ_{θ}^s is

$$\begin{aligned} \sigma_{\theta}^s &= 3\sigma_2 + \phi \frac{(1-2\mu)}{2(1-\mu)} (p_i - p_p) + p_{\pi} - \sigma_1 \\ &\quad + \frac{E\alpha_m}{3(1-\mu)} [T_w - T_0] - p_i - \varphi_c p_i. \end{aligned} \quad (18)$$

2.10. *Influence of Tectonic Stress and Overlying Stress on Fracture Pressure.* When the effective circumferential stress of the borehole wall rock σ_{θ}^s reaches the minimum tensile strength in the horizontal direction of the borehole wall rock S_t , the rock will fracture perpendicularly to the tensile stress direction [7].

$$\sigma_{\theta}^s = -S_t. \quad (19)$$

When the upper form is satisfied, $p_i = p_F$. p_F is the fracture pressure, MPa. If $K = \phi((1-2\mu)/2(1-\mu))$, (18) can be written as

$$\begin{aligned} p_F &= \frac{1}{1-K+\varphi_c} \left(3\sigma_2 - \sigma_1 + S_t - Kp_p + p_{\pi} \right. \\ &\quad \left. + \frac{E\alpha_m}{3(1-\mu)} [T_w - T_0] \right). \end{aligned} \quad (20)$$

$\sigma_3 = S$ is the overlying stress acting on the vertical direction, which can be obtained from the density logging curve. The effective overlying stress σ_3' is

$$\begin{aligned} \sigma_3' &= \sigma_3 - p_p, \\ \sigma_3' &= S - p_p. \end{aligned} \quad (21)$$

According to Hafner [27], in gentle or infinite horizontal strata, horizontal ground stresses are shown in the following expressions:

$$\begin{aligned} \sigma_1' &= \frac{\mu}{1-\mu} \sigma_3' + \alpha \sigma_3' + p_p, \\ \sigma_2' &= \frac{\mu}{1-\mu} \sigma_3' + \beta \sigma_3' + p_p. \end{aligned} \quad (22)$$

σ_1' is the effective maximum horizontal stress, MPa; σ_2' is the effective minimum horizontal stress, MPa; α and β are stress coefficients of geological structure.

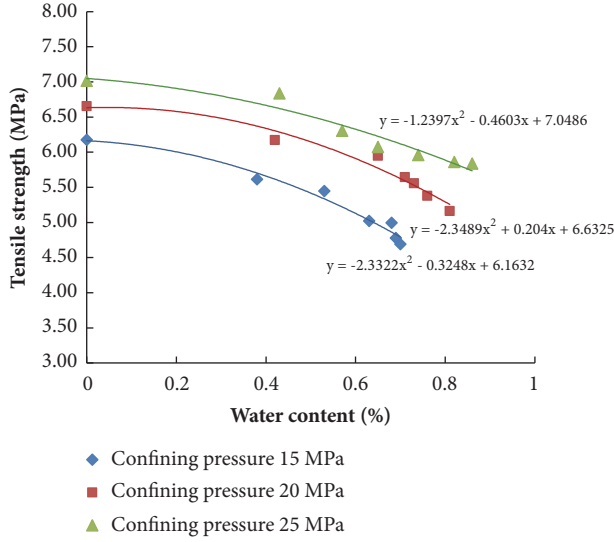


FIGURE 4: Relationship between tensile strength and water contents.

Submitting (22) into (20), p_F is obtained.

$$p_F = \frac{1}{1 - \phi \left(\frac{(1 - 2\mu)}{2(1 - \mu)} \right) + \varphi_c} \left(\left(S_t + p_\pi + \left(2 - \phi \frac{(1 - 2\mu)}{2(1 - \mu)} \right) p_p + \frac{E\alpha_m}{3(1 - \mu)} [T_w - T_0] \right) + \left(\frac{2\mu}{1 - \mu} + 3\beta - \alpha \right) S \right) \quad (23)$$

or

$$p_F = \frac{1}{1 - K + \varphi_c} \left(\left(S_t + p_\pi + (2 - K) p_p + \frac{E\alpha_m}{3(1 - \mu)} [T_w - T_0] \right) + \left(\frac{2\mu}{1 - \mu} + 3\beta - \alpha \right) \sigma'_3 \right). \quad (24)$$

3. Example Calculation of Rock Fracture Pressure Model

3.1. The Relationship between Tensile Strength and Water Contents. Qu et al. [6] carried out three axial compression tests of rock samples at different soaking time (see Table 1). According to previous tests, the tensile strength of rock is about 1/8~1/15 of compressive strength by Guo et al. [28]. According to the above conclusion, the tensile strength can be obtained by calculation (see Table 1).

The relationship between tensile strength and water contents is fitted as shown in Figure 4.

It can be seen from Figure 4 that the tensile strength decreases with the increase of water contents under different confining pressures. When there is high content of minerals in clays and micro cracks, the hydration will occur while the drilling fluid contacts them; in the meantime, the hydrated pores increase. Finally, the internal structure becomes looser,

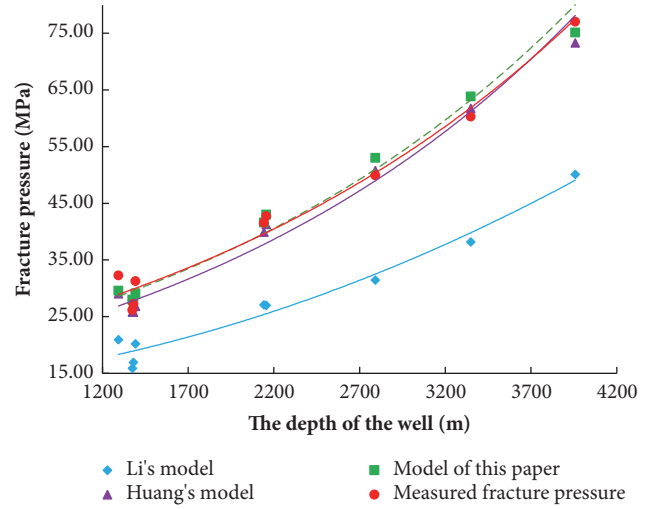


FIGURE 5: Variation of fracture pressure with depth in Dagang Oilfield.

the micro cracks expand, and the mechanical properties of rock will be reduced.

3.2. Example of Formation Fracture Pressure Calculation. By the performance parameters of strata, measured in situ stresses, and fracture pressure values in Dagang Oilfield [7, 18, 19, 25], the basic parameters of rock are selected as shown in Table 2. By (23), the calculated results of formation fracture pressure are shown in Table 3 and Figure 5.

From Figure 5, we can see that the formation fracture pressure increases with the increase of well depth. The fracture pressure calculated by the model in this paper is closest to the measured fracture pressure. By calculation, the error of the fracture pressure calculation model in this paper is 4.39%, while the prediction error of Li's model is 36.48% and 8.04% for Huang's model.

In this paper, a comprehensive model to calculate the rock fracture pressure by the theory of double effective stress of porous medium is established, which fully considers the deformation mechanism and material structure of the porous medium. It takes into account the stress field of wall rock, overlying stress, structural stress of inhomogeneous formation, additional stress caused by drilling fluid seepage, hydration stress, and temperature change stress caused by wellbore temperature difference and improves the calculation accuracy of fracture pressure. Therefore, it is more practical to calculate the equivalent drilling fluid density by this model.

Meanwhile, it can be seen from Figure 5 that the predicted values of fracture pressure are very close to the measured values in the well below 2900 meters, while it is slightly higher than the measured value in the section above 2900 meters. The reason is that the temperature change at the initial stage of cyclic injection drilling has a significant effect on the change of fracture pressure. After a certain period of cyclic time, the wall temperature is basically in the balance state and no longer affects the fracture pressure. The present study takes into account the effect of temperature variation in the whole

TABLE 1: Results of three axial compression tests of rock cores with different water contents [6].

Confining pressure	Soaking time/d	Water content $\omega_c/\%$	Compressive strength σ_s/MPa	Poisson ratio μ	Tensile strength S_t/MPa
15MPa	0	0	92.63	0.2	6.18
	0.5	0.38	84.21	0.18	5.61
	1	0.53	81.675	0.25	5.45
	2	0.63	75.35	0.2	5.02
	3	0.68	74.915	0.27	4.99
	4	0.69	71.65	0.2	4.78
20MPa	5	0.7	70.38	0.31	4.69
	0	0	99.83	0.3	6.66
	0.5	0.42	92.58	0.2	6.17
	1	0.65	89.23	0.26	5.95
	2	0.71	84.67	0.22	5.64
	3	0.73	83.355	0.31	5.56
25MPa	4	0.76	80.69	0.21	5.38
	5	0.81	77.435	0.21	5.16
	0	0	105.22	0.21	7.01
	0.5	0.43	102.52	0.2	6.83
	1	0.57	94.565	0.23	6.30
	2	0.65	91.1	0.19	6.07
	3	0.74	89.365	0.24	5.96
	4	0.82	87.91	0.18	5.86
	5	0.86	87.54	0.25	5.84

TABLE 2: Conventional parameters of rock formation.

Membrane permeable Efficiency I_m	Gas constant R'	Absolute Temperature T/K	Partial molar volume of pure water \bar{V}	The liquid activity of water entering the formation $(A_w)_m/m^3 \text{mol}^{-1}$
0.1	8.314	363	1.8×10^{-5}	0.78
the activity of water in formation $(A_w)_{sh}$	Rock porosity ϕ	Poisson ratio μ	Structural stress coefficient α	Structural stress coefficient β
0.915	0.18	0.22	0.91	0.31

well segment, so the predicted value of this well segment is a little higher.

Furthermore, the parameters of shale such as the elastic modulus are greatly influenced by temperature changes; the elastic moduli of rock above and below 2900 meters are different. In order to facilitate the calculation, the same value is adopted in the present study, which led to the deviation of the predicted value in the strata over 2900 meters.

3.3. *The Effect of Water Content on Fracture Pressure.* Combining the fitting formula of tensile strength and water contents in Figure 4 with (23), the relation diagram of rock fracture pressure and water contents is obtained (see Figure 6).

From Figure 6, we can see that the fracture pressure decreases with the increase of water contents. This is because water can soften the rock and change the mechanical properties of rock by hydration. Specifically, when the drilling fluid meets the clay minerals and micro cracks, the hydration effect will make the pore increase and loosen the internal structure of the rock, result in the propagation of the micro

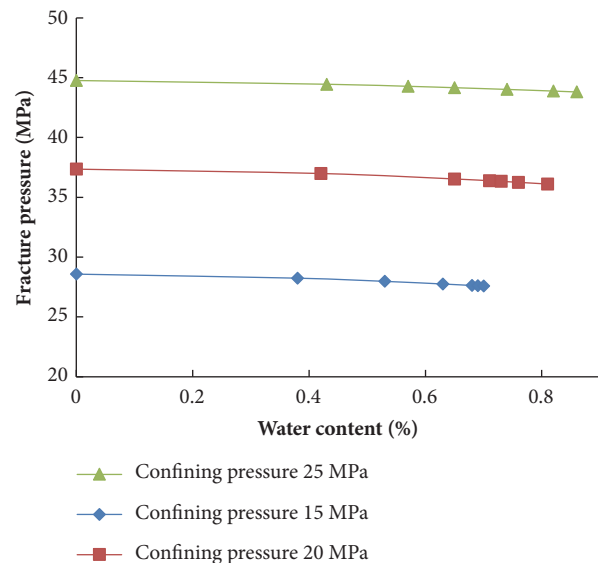


FIGURE 6: Relationship between fracture pressure and water content.

TABLE 3: Crustal stress and fracture pressure in oil formation in Dagang Oilfield.

Well No.	Average depth of well / m	Stratum pressure P_p /MPa	Tensile strength S_t /MPa	Effective overlying stress σ_3 /MPa	Minimum horizontal effective ground stress σ_2 /MPa	Maximum horizontal effective crustal stress σ_1 /MPa	Measured fracture pressure	Li's model	Huang's model	The present study
X814	1293	11.17	7.84	15.48	12.74	24.99	32.24	14.32	28.05	29.58
G662	1375	12.35	2.94	16.27	10.00	19.11	26.16	8.92	24.79	27.95
G772	1381	12.15	2.94	16.56	11.17	21.36	27.24	9.86	24.76	27.81
Y811	1393	12.25	3.92	16.66	13.13	24.30	31.26	12.71	26.45	29.06
B842	2792	24.60	2.94	35.86	22.34	44.68	49.88	16.12	48.48	53.02
B888	3349	29.59	3.92	43.61	26.75	53.50	60.26	19.59	58.98	63.85
B46	3958	34.88	3.92	53.11	33.32	61.73	77.02	27.45	69.83	75.12
H114	2142	18.42	3.92	27.14	18.23	34.98	41.55	15.49	38.20	41.59
H115	2156	19.01	4.90	26.85	17.83	34.69	42.72	15.51	39.59	42.98

crack, and finally decrease the mechanical properties of rock. With the increase of water contents, the compressive strength and tensile strength of rock reduce and then it leads to the decrease of fracture pressure.

4. Conclusions

(1) Based on the theory of double effective stress of porous medium, elastoplastic mechanics, rock mechanics, and the maximum tensile stress criterion, a comprehensive model to calculate the rock fracture pressure suited for different types of rocks is established in this paper.

(2) The fracture pressure model proposed in this paper takes into account the important effective factors: the crustal stress, the hydration stress, the temperature stress, the tectonic stress, the contact porosity of rock skeleton, the porosity of formation, and additional stress generated by seepage of drilling fluid. The calculation accuracy is improved for the prediction error which is 4.39%, which shows better agreement with the measured fracture pressure than other models.

(3) The effects of water contents on the tensile strength and fracture pressure are analyzed. Results show that both the tensile strength and fracture pressure decrease with the increase of water contents, which is due to the reduction of the mechanical properties of rocks by hydration.

Data Availability

The data used to support the findings of this study are available from the corresponding author upon request.

Conflicts of Interest

The authors declare that there are no conflicts of interest regarding the publication of this paper.

Acknowledgments

The present work is supported by the National Science Foundation of China under Grants Nos. 51674200, 51704233, and 51704237. Thanks are due to my daughter Xu Enyu especially.

References

- [1] T. Bu and P. Dai, "A simplified method of fluid-solid coupling simulation to stress-sensitive reservoir," *Journal of Southwest Petroleum University*, vol. 29, no. 4, pp. 145–147, 2008.
- [2] X. J. Liu and P. Y. Luo, "Study on the stability of well in mudstone strata," *Natural Gas Industry*, vol. 17, no. 1, pp. 45–48, 1997.
- [3] P. Wang, Z. Qu, H. Huang et al., "Creep Experimental Study of Brittle Shale Triaxial State under Aqueous," *Science Technology & Engineering*, vol. 16, pp. 66–71, 2016.
- [4] S. G. Li, J. G. Deng, B. H. Yu et al., "Formation fracture pressure calculation in high temperatures wells," *Chinese Journal of Rock Mechanics & Engineering*, vol. 24, no. 2, pp. 5669–5673, 2005.
- [5] V. Maury and A. Guenot, "Practical advantages of mud cooling systems for drilling," *SPE Drilling & Completion*, vol. 10, no. 1, pp. 42–48, 1995.
- [6] Z. Qu and P. Wang, *Creep damage Instability Study of shale*, Science press, 2016.
- [7] R. Huang, "A model for predicting formation fracture pressure," *Journal of the University of Petroleum China*, no. 4, pp. 16–28, 1984.
- [8] W. Zhang, S. Deng, H. Fan et al., "3D Calculation and Display for Formation Fracture Pressure," *Science Technology & Engineering*, vol. 2, no. 1, pp. SB57–SB68, 2014.
- [9] R. A. Anderson, D. S. Ingram, and A. M. Zanier, "Determining fracture pressure gradients from well logs," *Journal of Petroleum Technology*, vol. 25, pp. 1259–1268, 1973.
- [10] C. L. Li and X. Kong, "A theoretical study on rock breakdown pressure calculation equations of fracturing process," *Oil Drilling & Production Technology*, vol. 22, no. 2, pp. 54–56, 2000.
- [11] C. L. Li, X. Y. Kong, and Z. X. Xu, "Double Effective Stresses of Porous Media," *Nature Magazine*, vol. 24, no. 12, pp. 1515–1518, 1999.
- [12] B. Haimson and C. Fairhurst, "Initiation and extension of hydraulic fractures in rocks," *SPE Journal*, vol. 7, no. 03, pp. 310–318, 2013.
- [13] E. Detournay and R. Carbonell, "Fracture-mechanics analysis of the breakdown process in minifracture or leakoff test," *SPE Production and Facilities*, vol. 12, no. 3, pp. 195–199, 1997.
- [14] C. Jiao, S. He, Q. Xie et al., "An experimental study on stress-dependent sensitivity of ultra-low permeability sandstone reservoirs," *Shiyou Xuebao/Acta Petrolei Sinica*, vol. 32, no. 3, pp. 489–494, 2011.
- [15] P. Lu, Z. W. Sheng, and G. W. Zhu, "The Effective Stress and Mechanical Deformation and Damage Characteristics of Gas-filled Coal," *Journal of University of Science & Technology of China*, vol. 31, no. 6, pp. 686–693, 2001.
- [16] X.-L. Jiang and P.-C. Li, "Calculation of intergranular suction considering cementing area between soil particles," *Yantu Gongcheng Xuebao/Chinese Journal of Geotechnical Engineering*, vol. 38, no. 6, pp. 1160–1164, 2016.
- [17] X. Y. Yan, Y. Q. Hu, and N. Li, "Calculation model of breakdown pressure in shale formation," *Lithologic Hydrocarbon Reservoir*, vol. 27, no. 2, pp. 109–113, 2015.
- [18] J. Deng, "Formation Fracture Pressure Prediction Method," *Petroleum Drilling Techniques*, vol. 37, no. 5, pp. 43–46, 2009.
- [19] H. Rouse, "Elementary Mechanics of Fluids," 1946.
- [20] X. J. Zhao, Q. Zhan, H. Fan, H. B. Zhao, and F. J. An, "Cracking mechanism of shale cracks during fracturing," *IOP Conference Series: Materials Science and Engineering*, vol. 372, p. 012046, 2018.
- [21] T. Liu, P. Cao, and H. Lin, "Evolution Procedure of Multiple Rock Cracks under Seepage Pressure," *Mathematical Problems in Engineering*, vol. 2013, Article ID 738013, 11 pages, 2013.
- [22] P. Suraneni and R. J. Flatt, "Micro-reactors to study alite hydration," *Journal of the American Ceramic Society*, vol. 98, no. 5, pp. 1634–1641, 2015.
- [23] J. Gui, T. Ma, P. Chen, H. Yuan, and Z. Guo, "Anisotropic Damage to Hard Brittle Shale with Stress and Hydration Coupling," *Energies*, vol. 11, no. 4, p. 926, 2018.
- [24] M. E. Chenevert and V. Pernot, "Control of Shale Swelling Pressures Using Inhibitive Water-Base Muds," in *Proceedings of the SPE Annual Technical Conference and Exhibition*, New Orleans, Louisiana, 1998.
- [25] M. B. Boas, "Temperature Profile of a Fluid Flowing within a Well," in *Proceedings of the SPE Latin America Petroleum*

Engineering Conference, pp. 439–446, Rio de Janeiro, Brazil, 1992.

- [26] V. Hooker and W. Duvall, “In situ rock temperature-stress investigations in rock quarries,” *Ntis Pb*, 1971.
- [27] W. Hafner, “Stress distributions and faulting,” *Geological Society of America Bulletin*, vol. 62, no. 4, pp. 373–398, 1951.
- [28] J.-C. Guo, Z.-H. Zhao, S.-G. He, H. Liang, and Y.-X. Liu, “A new method for shale brittleness evaluation,” *Environmental Earth Sciences*, vol. 73, no. 10, pp. 5855–5865, 2015.



Hindawi

Submit your manuscripts at
www.hindawi.com

